Bar-Ilan–Yeshiva University

Summer Science Research Internship Program 2021

The Bar-Ilan University–Yeshiva University Summer Science Research Internship Program is an amazing research opportunity for undergraduate men and women, allowing them to contribute to the forefront of science research taking place in Israel. Generously supported by former chairman of Bar-Ilan's Global Board of Trustees, Dr. Mordecai D. Katz z"l and his wife Dr. Monique Katz, and by the Barbara and Fred Kort Foundation, students gain invaluable laboratory skills, along with an unforgettable summer experience.

Program Director: Prof. Arlene Wilson-Gordon

Av and Em Bayit: Rav Chaim and Ronit Goldberg

TABLE OF CONTENTS

Editor: Sarah Liberow
Contributing Editor: Mili Chizhik

BRAIN SCIENCES

(L-R) Aaron Purow, Rami Nordlicht, Ari Englander, Alyssa Silvera, Sara Evans, Chaya Bracha Gordon, Shira Joshua

The Use of Magnetoencephelography in Brain Studies

Ari Englander

Advised under Prof. Avi Goldstein and Barak Atia

Magnetoencephalography (MEG) is an innovative, non-invasive neuroimaging technique. As opposed to electroencephalography (EEG), which measures the electrical activity of the brain, MEG measures the magnetic oscillations from the brain, allowing the detection of brain activity in temporal resolution of milliseconds and spatial resolution of millimeters. The acquisition of brain activity is conducted by whole-head, 248-channel magnetometer array (4-D Neuroimaging) in a magnetically shielded room with a sampling rate of 1017Hz. MEG does not produce an anatomic image of the brain; thus, an anatomical MRI image of each subject is needed to analyze the source of activity in the brain. Ideally, every subject will have their own unique MRI scan to more precisely pinpoint the source of brain activity. Unfortunately, most studies can't afford to conduct an MRI scan for each subject. In these instances, a sample MRI template is used. When an MRI template is used, it needs to be resized and adjusted to fit the subject's head size. Therefore, the size of every subject's head is measured at the beginning of the MEG experiment. The entire analysis of the data was

performed using Matlab® R2013b and FieldTrip toolbox for MEG analysis (Open Source Software for Advanced Analysis of MEG, Oostenveld et al., 2011).

As part of my internship at the MEG lab at Bar-Ilan University, I took part in analyzing two different experiments. The first experiment deals with food perception, and the main question of the experiment is whether images of high-calorie food engage different brain areas than images of low-calorie food. The second experiment studies former soldiers, and examined their brain activity in response to several cognitive tasks. More specifically, I helped to resize and realign the MRI templates and create a unique file that fits each subject individually. In addition, I helped to create and produce several necessary files for the next step of source analysis in the brain. Finally, I experimented with calculating the source analysis of the MEG signals.

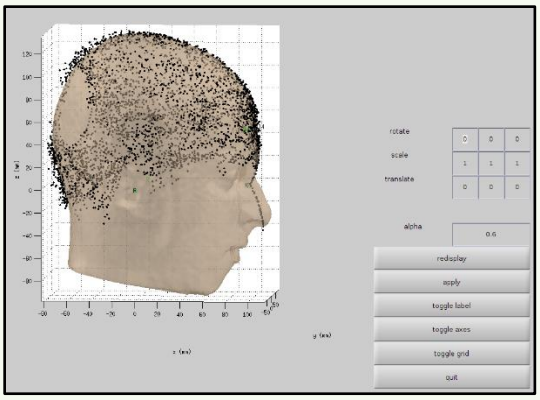

Figure 1: Combined MRI and MEG scans.

Parkinson's Disease and Emotional Regulation

Sara Evans

Advised under Dr. David Anaki

Parkinson's disease (PD) is a neurodegenerative neurological disease, meaning that over time the symptoms get worse and are irreversible. The most common first sign of Parkinson's is a resting tremor, which typically intensifies with stress or excitement. Yates says that the first thing to typically go is the olfactory sense since the, "degeneration starts in the dorsal motor nucleus of the vagus and the anterior olfactory structures." After this the raphe nuclei along with the locus coeruleus is affected and next the substantia nigra, amygdala, and nucleus basalis of Meynert. This stage of deterioration is what leads to the motor dysfunction that we associate with Parkinson's disease. As the disease progresses the temporal lobe mesocortex is deteriorating along with the parahippocampal cortex and then the neocortex. The final stage is when "the neocortex areas of the primary sensory function and motor areas show degeneration" (Yates, 2019, p.673). Almost all symptoms are due to a dopamine deficiency. Individuals with Parkinson's disease experience cognitive decline and impairments with emotional regulation. This can have detrimental effects on the person's quality of life and is therefore studied to see the impact it has.

A meta-analysis is a compilation of different studies regarding one shared topic. In the case of Parkinson's disease and emotional regulation there have been many correlational as well and comparative studies conducted over the years. The reason meta-analysis is important for this topic is because many people diagnosed with PD suffer from issues with emotional regulation (ER), but it is not as widely known. Therefore, it is important to increase awareness of the issue to better understand the disease and how it affects an individual. Using various databases such as ProQuest, PubMed, and Scopus along with specific word searches a total of 26 relevant papers from 1990-2020 were found. In the comparative studies emotional regulation abilities were measured against a control group. In the correlational studies there was only an experimental group, the individuals with PD. The ability to emotionally regulate oneself was

compared using TAS (Toronto Alexithymia Scale), COPE (Coping Orientation to Problems Experienced), or one of a few other forms of measurements. After looking through all the relevant articles they were organized and put into an excel file showing all the different data points.

References:

Yates, J. R. (2019). Chapter 20, Neurodegenerative Diseases. In J. S. Meyer & L. F. Quenzer (Authors), *Psychopharmacology: Drugs, the brain, and behavior* (pp. 671-695). Sunderland, MA: Sinauer Associates.

Molecular Correlates of Separate components of Training that lead to memory formation in *Aplysia*

Chaya Bracha Gordon

Advised under Prof. Abraham Susswein and Dr. Yisrael Schnytzer

Molecular correlates of learning in the marine gastropod opisthobranch mollusk, *Aplysia*, are a topic of interest and are investigated to better understand the specific genes involved in memory formation. It is well established in the scientific literature on memory that certain transcription factors are associated with memory formation such as C/EBP and CREB1. In *Aplysia*, CREB1 is further processed to produce CREB1α and CREB1β which, like the other transcription factors, turn on other genes that will then transport their mRNA from the nucleus to the synapses to produce long-term changes that take place later during memory consolidation.

Aplysia is a well-established model for studying learning due to its large neurons and ability to form both long-term and short-term memories in response to a stimulus. The Nobel prize has been awarded for work done to study molecular correlates of memory in *Aplysia*. Therefore, to investigate the molecular correlates of learning in this organism, the animals were trained to learn whether a specific food was edible or not. This associative learning task contained three conditions that are necessary for memory formation including (a) lip stimulation with a specific food; (b) attempts to swallow the food; (c) failure of the food to enter the gut. In addition, to identify the effect of lip stimulation alone, one group of animals received lip stimulation but were prevented from biting. By separating the components of learning, the different molecular correlates could be identified.

In previous research, CEBP expression was found to increase in the sensory cells of the buccal ganglia after a full training. Given that the buccal ganglion has a primarily motor function, this was interesting to note. Later, correlates of the connectivity between buccal ganglion sensory cells and motor neurons were found in trained versus naive animals. In trained animals, increased connections between the buccal ganglion sensory cells and the neurons responsible for protraction, which is used when rejecting food, were found. The opposite was seen to be true in untrained animals with the sensory cells formed stronger connections with neurons associated with retraction, which is used when ingesting food. Therefore, sensory cells have molecular and physiological correlates of learning present.

Although this did afford some knowledge of learning in Aplysia, there are still lacking molecular correlates of learning in the cerebral ganglia, and there are indications to assert that some changes in behavior that result from learning are localized to this ganglion. To this end, animals were trained according to previous protocols. After training, the ganglia were excised from the animals both 15 minutes and 2

hours subsequent to training to ensure coverage of possibly early or late peaks in gene expression. Total RNA was then extracted from the cerebral and buccal ganglia, followed by cDNA synthesis and then quantification of gene expression by qPCR. In total, there were five experimental groups: trained and dissected after 15 minutes, trained and dissected after 2 hours, lip stimulation and dissected after 15 minutes, lip stimulation and dissected after 2 hours, and naive animals. Currently, the data is being optimized to better understand the story surrounding molecular mechanisms important in *Aplysia*.

Masked Communication

Shira Joshua

Advised under Dr. David Anaki

Throughout the duration of the COVID-19 pandemic, many countries required the use of face masks in all public locations. Masks cover most people's faces, leaving only the forehead and eyes visible. The study conducted analyzed the potential impact that masks have on people's perception and recognition of facial expression.

Previous studies have shown that it is harder to detect emotions relying solely on the eyes. This experiment intended to test those findings in relation to the COVID-19 pandemic. In the experiment, we presented five different conditions of individuals: full face; half face; mask on chin, only; face mask; and scarf. For every condition we presented six emotions: happiness, sadness, anger, fear, disgust and neutral. The recognition of emotions in facemask and full face conditions were compared between the different participants and analyzed for replication purposes. In addition, this experiment would address the question whether the type of mask used influences facial emotion perception by comparing the half face condition to the scarf and face mask conditions. Additionally, we hypothesized that the mask condition would be associated with COVID-19 related emotions such as fear or disgust.

The experiment was conducted by E-prime. In total there were 720 different pictures divided into 4 separate studies of 180 pictures each. Each version would randomly assign each picture in an order. We recruited N=40 young adults: half women and half men. The pictures were presented on a screen and participants had to select what they perceived as the correct emotion. Participants came to the lab and took the experiment in a quiet room accommodated for experimental procedures. Those who were not able to come to the lab took the experiment on their own via a laptop in various places.

Results presented a difference of 0.095 for emotional recognition between full face and a cover: bandana, mask, half face, (Figure 2). In combining all conditions together, the scale presents the following expressions from high to low: happy, neutral, fear, anger, sad and disgust (Figure 3). With the mask condition (Figure 4), the expression of happiness was the easiest to detect, while fear was second and disgust was last. Prediction for the mask condition was to be associated with COVID related emotion such as fear and disgust. In fact, fear was highly correlated with masks, however, disgust scored the lowest average. Additionally, it is interesting to note that on average, disgust emotion was significantly lower than the other expressions (Figure 1).

Figure 1

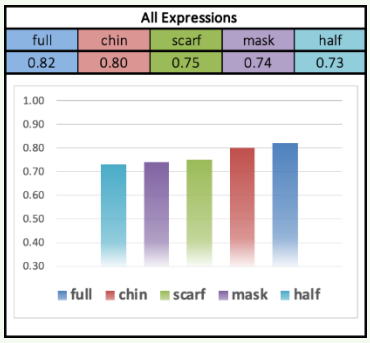

Figure 2

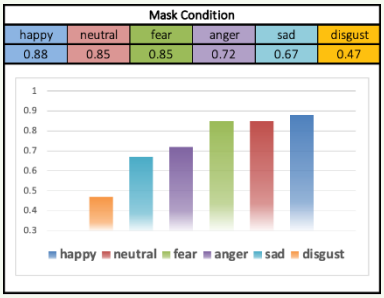

Figure 3

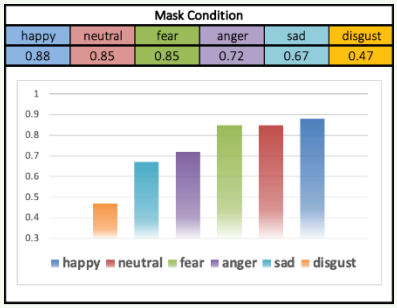

Figure 4

The Interface Between the Olfactory System and Learning and the Relationship Between Task Difficulty and Retention

Rami Nordlicht

Advised under Dr. Rafi Haddad

Almost all animals, even those with seemingly rudimentary cranial structures and nervous systems, have shown the ability to engage in associative learning, or the ability to recognize patterns and relationships between external stimuli. In many mammals, including rodents, the predominant sense used to detect and analyze the environment is olfaction. In the mammalian olfactory system, airborne molecules dissolve in the mucus surrounding olfactory receptors, which line the olfactory epithelium in the dorsal nasal cavity. The binding of an odorant to the receptors results in the depolarization of the nerves surrounding the receptors, and the resulting action potential is sent to the olfactory bulb via the olfactory nerve where signals are sorted by glomeruli and are eventually projected to the insula and the orbitofrontal cortex. Because olfactory systems are used by systems involved with learning and memory, animals like mice that display extensive dependence on their sense of olfaction can be used as excellent models to show the relationship between olfaction sensitivity and learning, and an experiment was designed to analyze the way mice use olfaction to learn and form nondeclarative memories using classical conditioning and ultimately investigate how odor information is processed in different subregions of the olfactory cortex.

The experimental setup consisted of water filled into a test tube that could be automatically dispensed simultaneously with one or both of two odorants that had been prepared and stored in a centrifuge tube into a small hole in a cage. The water tube was positioned at least 3 cm away from the cage's opening, as during the more advanced stages of the experiment, the additional effort required by the mice to obtain a droplet of water would serve as the negative stimulus. When an experimental water-deprived mouse would approach the hole at which the

water and odorant tubes were oriented, a motion sensor would detect the mouse's presence, which would in turn trigger the release of an odorant, and depending on the stage of the experiment, a droplet of water. The effort required by the mice was manually increased as they gradually grew more familiar with the setup. During basic training, water was released simultaneously with both odorants. Once familiarized with water source, a second training module was used such that water would only be released in tandem with the positive stimulus odorant; the water tube remained dry during the release of the negative stimulus odorant. Finally, once the mice were sufficiently familiar with the positive stimulus odorant such that they reacted to the positive stimulus and avoided the negative stimulus over several hundred trials spanning a few days, a third module was used in which the mice would only receive a droplet of water with the release of the positive stimulus and only once sensors on the water tube detected that the mouse had tried to lick the tube. In other words, while during the second training module, the mice could have theoretically used their auditory or visual senses to detect the presence of water, the third module ensured that the mice were using their olfactory senses to obtain the water droplet.

In addition to the increasing effort required by the mice to receive their reward as the experiment progressed, the odorant stimuli used in the experiment were also made increasingly difficult to discriminate. In the first stages of training, the experimental mice needed to distinguish between the scents of orange and mint in order to receive a reward, but, as the experiment progressed, the mice ultimately were required to distinguish between two solutions, one consisting of 53% ethyl acetate and 47% isoamyl acetate and the other consisting of 53% isoamyl acetate and 47% ethyl acetate, in order to obtain a droplet of water.

Over the course of the experiment, the mice were shown to gradually learn the differences between the two odors and overwhelmingly only exerted effort to reach the droplet of water upon the release of the positive odorant stimulus. Moreover, the mice were shown to be able to remember the differences between the two odorants over the course of several weeks, regardless of the difficulty in discriminating between the two odorants. Further anatomical analyses of the experimental olfactory bulbs are needed to sufficiently analyze underlying neuronal connections and communication.

Brain Multiplicity and the Modal Model

Aaron Purow

Advised under Professor Eshkol Rafaeli

When speaking about cognition, there is this illusion which presents that our minds are in a position of unitary selfhood in that they are occupying only one current cognitive state. However, our minds are occupied in many states, characters, identities, self-positions, and voices concurrently in a phenomenon known as multiplicity. Additionally, within the realm of cognition and self-concept there is a distinction between the "me" and "I". The "Me" refers to the objective declarative knowledge about oneself, while the "I" refers to the subjective experience one captures from the first-person perspective. Originally, "I" and "me" were seen as one in the same within one's unitary view of self but the multiplicity was then studied within the realm of "me" and captured its complex structure. Little multiplicity has been studied in regard to the "I". Professor Rafaeli seeks to explore the multiplicity within the realm of "I".

Professor Rafaeli was inspired by the Schema Therapy Model which is a young practice proposed by Jeffery Young in 1990 and serves as

an extension to the well-known cognitive behavioral therapy (CBT). It was introduced as CBT was less effective with some patients (e.g. patients with personality disorders) and also would result in consistent relapse after treatment. So therefore, Young introduced a method which instead of dealing with surface level cognitions/behaviors dealt with deeper mental constructs. Schema Therapy especially is beneficial for people dealing with longer standing emotional/relational difficulties which are common in people with various personality disorders. This is especially true as certain maladaptive schemas can emerge from prior core emotional needs going unmet which can lead to current day obstructive behaviors in a concept referred to as "maladaptive coping styles".

While the schema therapy model originally focused on the study of general needs, schemas, and coping mechanisms, it later became more personalized. The modal model was born which breaks up schemas into various modes which are said to interact to impact one's overall psychological construct. The modal model fits well with the idea that people's cognition consistently changes based off current external factors. There exist 4 categories of modes which include child modes, coping modes, introjected modes, and healthy modes. Professor Rafaeli seeks to specifically study multiplicity of modes among both typical adults and ones who are suffering from anxiety disorder in order to bridge the gap between modal theory and clinical practice. The study has three parts. Part 1 studies the modal differences and similarities between regular people without test anxiety and people with test anxiety. Part 2 demonstrates the association between self-reported and observed modes and how modes change with therapy intervention. And finally, part 3 seeks to explore common characteristics in each of the mode categories by priming participants to experience the four different mode categories. One of the characteristics being used in part 3 included heart rate variability (HRV) and electrodermal activity (EDA) as HRV levels are predicted to be the highest in the participants primed to experiencing the healthy mode while EDA levels are predicted to be the highest in the participants who are primed to experiencing the vulnerable child mode. This is because HRV and EDA analysis can serve as objective measurements for arousal and therapist patient synchrony. For the short time we spent here over the summer, I was privileged with the task of going through the EKGs and EDAs to clean the data and determine whether they were clean enough to be used. The overall benefits of the modal model will increase with its continued research. The modal model introduces us to the various ways one can respond to a unique situation in a very personalized way, allows us to reflect on one's psychological construct beyond one's surface level thoughts and actions, and allows one to select a mode most conducive to different situations.

Turner's Syndrome and Social Cognition

Alyssa Silvera

Advised under Dr. David Anaki

Turner's syndrome (TS) is a chromosomal disorder that affects 1 out of 2,000 females characterized by a partially or completely absent X chromosome [1,2]. While most people have 46 chromosomes, women with Turner's Syndrome usually have 45. Named after Henry Turner, an endocrinologist who discovered the syndrome in 1938, Turner's syndrome is associated with various physical abnormalities including short stature, webbed necks, cardiac and renal defects as well as ovarian dysfunction which leads to estrogen deficiency and infertility. In addition to

physiological symptoms, Turner's syndrome manifests itself through cognition as well. Individuals with Turner's syndrome demonstrate typical intelligence and verbal skills; however, they experience deficits in visuospatial and motor skills, executive functions, mathematics, and language. They also demonstrate poor psychosocial functioning which can be expressed through difficulties in forming and maintaining social relationships.

The present meta-analysis was conducted to assess the relationship between Turner's syndrome and social cognition. Social cognition can be described as the mental processes involved in perceiving and attending to the other people in our social world. Individuals with Turner's syndrome have shown significant impairments in face perception as well as Theory of Mind (ToM), which is the ability to attribute mental states to the intentions of others' behaviors. These deficiencies are generally attributed to neuroanatomical anomalies in the hippocampal and amygdalar regions of the temporal lobe found in women diagnosed with Turner's syndrome.

References:

[1] Anaki, D., Zadikov Mor, T., Gepstein, V., Hochberg, Z; (2016). Face perception in women with Turner syndrome and its underlying factors. Neuropsychologia, 90, 274–285. https://doi.org/10.1016/j.neuropsychologia.2016.08.024

[2] Kesler, S. R., Garrett, A., Bender, B., Yankowitz, J., Zeng, S. M., & Reiss, A. L. (2004). Amygdala and hippocampal volumes in Turner Syndrome: A high-resolution MRI study of x-monosomy. Neuropsychologia, 42, 1971–1978. https://doi.org/10.1016/j.neuropsychologia.2004.04.021

LIFE SCIENCES

(L-R) Shani Adest, Sarah Liberow, Eliana Farkas, Eden Shweky, Tova Wax, Leeba Sullivan, Michael Akhavan

Unraveling RNA dynamics under HSV-1 infection

Shani Adest

Advised under Prof. Yaron Shav-Tal and PhD student Shani Nadav

Herpes is a common virus with many strains. HSV-1 is the most common herpes virus which infects more than 67% of the population under the age of 30. The HSV-1 life cycle contains both a latent and a lytic phase. The latent phase infects the nerve cells as an extra chromosomal element, with most of the viral genome being silenced. The lytic phase is the active infection phase of the virus and contains several steps including penetration, viral gene expression,

replication, virion assembly, and release of new virions to adjacent cells. Replication and gene expression of the viral DNA is confined to distinct intranuclear sites known as Viral Replication Compartments (VRCs). Transcription of mRNA needs to undergo maturation in order to be exported out of the nucleus for translation. One of the most important maturation processes the mRNA transcript needs to undergo is splicing. Splicing is performed by the 'Spliceosome' in which the introns are removed, and the exons are fused together. The spliceosome is a complex of RNA and proteins. The spliceosome components and other splicing factors are found in nuclear bodies called nuclear speckles. There is a controversy among scientists regarding the role nuclear speckles may play in the splicing process. Some scientists theorize that the speckles act as a storage site for splicing factors and their proteins migrate to an active gene in which the mRNA needs to be spliced. Other scientists theorize that the speckles stay together as a nuclear body and are localized in proximity to active genes, where they are needed for mRNA splicing. Our research is performed under the assumption that the first model is the correct theory.

We used cell staining techniques to see the location of speckles in uninfected cells as well as in cells infected with HSV-1 virus. In healthy cells, speckles are spread out in the nucleus. However, in HSV-1 infected cells the speckles were found surrounding the periphery of the VRC's, a phenomenon known as localization at the periphery of the nucleus (Figure 1). Our study aims to determine why this phenomenon happens with the speckles. It is theorized that it may be related to the export of the virus, however the full function and reasoning has yet to be determined.

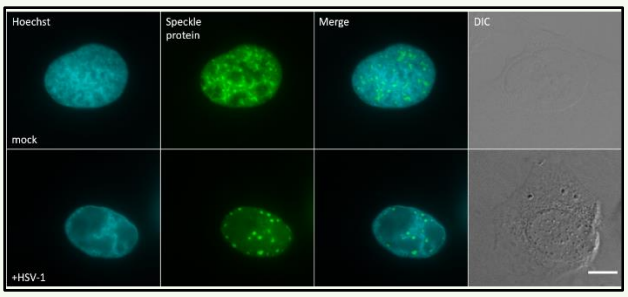

Figure 1: Infected cells with VRCs and speckles in the VRCs

When we stained the cells with probes to detect the viral mRNA in the cells, we were able to see the viral mRNA in the VRCs (Figure 2). We used three different mRNA probes to detect three different viral mRNA. The HSV-1 virus replication cycle has different stages, with different proteins added at each stage. The first two viral mRNA we stained were immediate early genes in the cycle, while the third viral mRNA was a late-stage gene. As the hours post infection increases, the mRNA aggregated into large clusters which co-localize with the VRCs. The VRC's are where viral gene expression takes place, therefore it makes sense that there are many viral mRNA found in these sites.

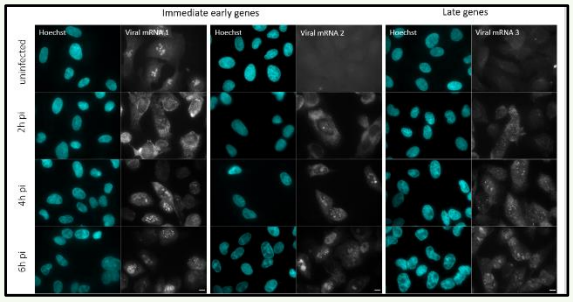

Figure 2: Three different viral mRNA in HSV-1 infected cells

By the end of the infection, we observed in viral mRNA 1 and 2 bright foci of mRNA at the periphery of the nucleus that look like nuclear speckles. Additionally, when we also stained the speckles we see a complete co-localization between the speckles and the viral mRNA foci in viral mRNA 1 and 2 but not in 3 (Figure 3).

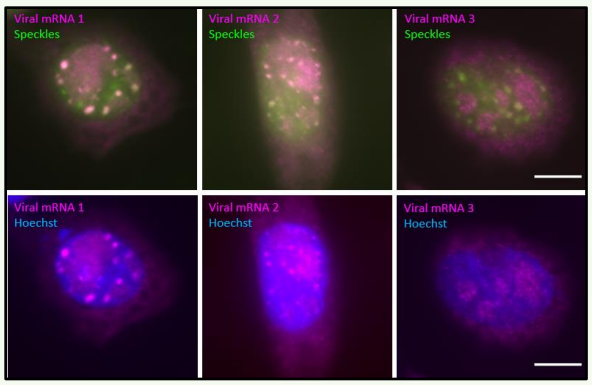

Figure 3: Viral mRNA localization in nuclear speckles

Viral mRNA 1 and viral mRNA 2 are both immediate early genes however, viral mRNA 3 is a late gene, which can explain the difference between them regarding their localization to the speckles. It is still unknown why this occurs. It may be that some mRNA was already transcribed earlier and moved to speckles, and the newer ones are in the VRC's but have not been transferred to the speckles yet. In viral mRNA 3, which is a late stage gene, perhaps more time needs to pass for the mRNA to go into the speckles, or maybe it is not needed in the late stage genes at all. All of these questions are being theorized and analyzed in our research.

The final experiment we are performing is to analyze how the mRNA acts when the nuclear speckles are dispersed. One way to perform nuclear speckle dispersion is to overexpress the Clk1 kinase. This kinase phosphorylates the speckles proteins enabling the speckles components to leave the speckle group to go to a specific gene. Studies have shown that overexpressing that kinase disassemble the nuclear speckles structures. Under these conditions we observed aggregation of mRNA in the cytoplasm (Figure 4). This is the first time we observed aggregation of viral mRNA in the cytoplasm, as opposed to in the nuclear periphery. It is still unclear why this occurs. The aggregation of viral mRNA in the cytoplasm resembles p-bodies, which are bodies in the cytoplasm that contain RNA for degradation. Therefore, a theory is that maybe the mRNA is going into the p-bodies to be degraded for some reason. It may be that they are not in p-bodies but some other structure that resembles p-bodies, for some other purpose. Our research aims to determine what is happening to the mRNA in the cytoplasm and why it aggregates there.

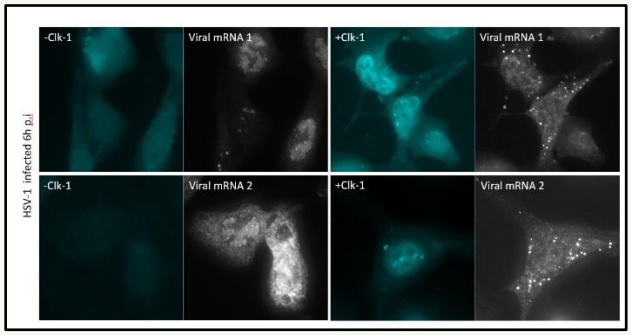

Figure 4: Viral mRNA under dispersion of speckle using CLK1

The future experiments of this research will include staining p-bodies in an attempt to understand the localization of viral mRNA in the cytoplasm under speckles dispersion conditions. The research will continue to try to answer the unknown related to the VRC's, speckles, and mRNA under infection conditions, as well as how they relate to each other.

Exploring the allosteric effects of the zinc finger in human SIRT6 protein

Michael Akhavan and Leeba Sullivan

Advised under Prof. Haim Cohen and Noga Tauitou

Longevity and healthspan are of universal interest and have many broad downstream applications. Research in these topics has made considerable strides in recent history. While many factors affect lifespan and healthspan, in recent years there has been a significant correlation between Sirtuin proteins and longevity, specifically Sirtuin 6. Sirtuin 6, or

SIRT6, is an NAD+ dependent protein deacetylase. SIRT6 can act both as an ADP-ribosyl transferase and histone deacetylase, playing a critical role in various metabolic cycles including gluconeogenesis, DNA repair, and lipid metabolism [1].

The effects of overexpression of SIRT6 have been connected to extending healthy lifespan through maintaining and restoring energy homeostasis. Recent literature has shown that the overexpression of SIRT6 lengthened the lifespan of mice by 23%, while also maintaining their healthspan. Furthermore, SIRT6 was shown to preserve hepatic glucose output and glucose homeostasis. These findings show that SIRT6 optimizes energy homeostasis in old age to delay frailty and preserve healthy aging [2]. As SIRT6 is a protein with a strong connection to a lengthened lifespan, the analysis of SIRT6 structure and function can contribute to further breakthroughs in the study of human aging.

In addition to the catalytic pocket, SIRT6, like many other proteins, contains a zinc finger, a structural motif on the Sirtuin. While little is currently known about the function of the zinc finger on SIRT6, it may play a crucial role in the proper folding of the protein or impede on its ability to successfully bind to its substrate, despite its large distance from the catalytic site of SIRT6.

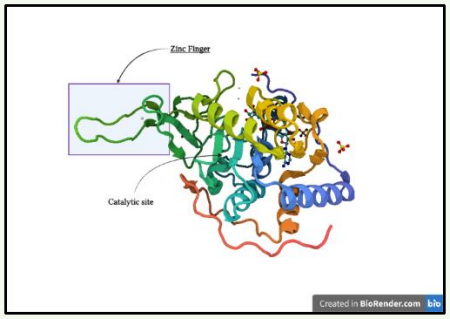

Figure 1: Structure of SIRT6 protein

Four cysteine residues of SIRT6 hold the zinc atom in place through various chemical interactions. To understand the importance of the zinc finger to the various protein interactions SIRT6 finds itself in, point mutations of the cysteine residues were created. Cysteine has a strong affinity for the Zn^{2+}, via the electrostatic interactions with the zinc and the sulfur atom of the residue. Manipulations of this zinc finger on a molecular level can likely provide significant insight into the function of the zinc finger within the broader picture of the Sirtuin molecules. Mutagenesis was used to exchange the cysteine residue with an arginine residue to remove the interactions between the sulfur atom and the Zn^{2+} ion [3]. Upon obtaining protein samples from the BL21 transformed E. Coli, with a mutation of the cysteine connected to the zinc finger, thermal analysis and activity assay were performed. After incubating the proteins at various temperatures from both the wildtype and mutant proteins, samples were run on a western blot to visualize the protein and its activity.

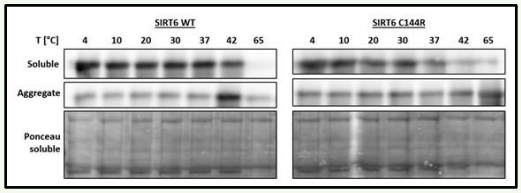

Figure 2: Thermal Analysis of the SIRT6 protein compared to that of the mutation

The mutant protein of SIRT6 had a much more significant protein degradation than the wildtypes which can be based on the gradient depicted in Figure 2. In addition, the mutant samples appeared to have significantly more protein aggregate present than the control, even at temperatures that the protein would normally be expected to be stable at, indicating the role of the cysteine residue in the native protein.

The proteins were then used for an activity assay to determine whether the mutation connecting to the zinc finger affected the enzyme's catalytic

activity despite its large distance from the active site. The assay was conducted at 30˚C due to the stability of the mutant protein based on the previous thermal analysis. As SIRT6 acts as a histone deacetylase, the acetylation of H3 K9a was monitored in the presence of SIRT6 as well as NAD+. Compared to the wildtype, which had increasing deacetylation activity over time, the mutant protein appeared to have no catalytic activity at the site of the histone as seen in Figure 3. Analysis of the blot using Image J enabled quantification of the catalytic activity of SIRT6. The normalized activity of the mutated SIRT6 was significantly depleted compared to that of the wildtype, as depicted in Figure 4.

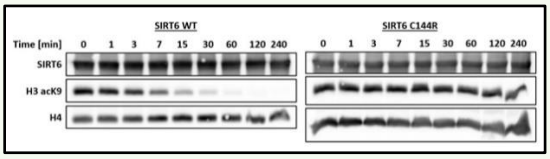

Figure 3: Activity assay of the mutant compared to the wild type in H3 acK9 and H4 histones

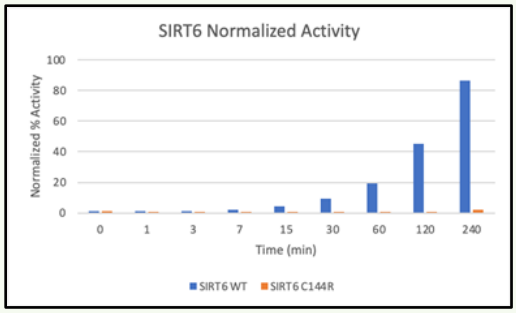

Figure 4: Normalized analysis of the SIRT6 wild type compared to the SIRT6 mutation using ImageJ

Further analysis of the other cysteine residues that interact with the zinc finger of SIRT6 would allow for further characterization of the protein. Additionally, mutations of the cysteine residue in the SIRT6 have been strongly correlated with thyroid cancer, providing additional interest in the protein mutation with potential for broader downstream cancer therapeutic effects [4]. The cysteine residue exchanged for tyrosine, a larger aromatic amino acid, depicted in Figure 5 has been found in various forms of thyroid cancer and may affect its native folding. The second mutation of interest was the removal of the thiol group from the cysteine residue, which is understood to have the strongest electrostatic interactions with the zinc molecule [3]. The exchange of the cysteine residue with an alanine residue via mutagenesis would allow us to determine if the sulfur molecules interact with the zinc finger.

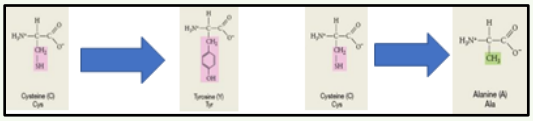

Figure 5: Amino acid structure of the two mutations

Mutagenesis was performed using obtained primers for the various mutations. The primers were then transformed into H2ka bacterial cells. To test the successful presence of the transformation and SIRT6 insert, a western blot assay was performed on multiple colonies. Restriction enzymes were used to test for the successful replication and transformation of the plasma inset which was present at approximately 1kb, as depicted in figure 6. The data shows that the SIRT6 insert was indeed successful. Further genomic sequencing and activity assays can give greater insight into the mutant protein, with potential for downstream medicinal effects.

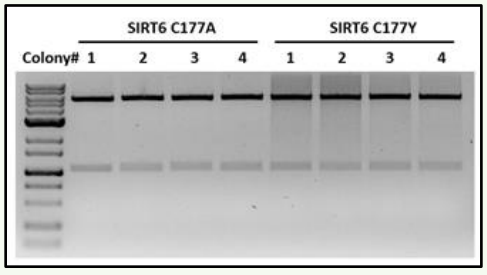

Figure 6: Mutations extracted from bacteria

Through our research, we were able to conclude that the zinc finger is indeed important in the various protein DNA interactions. When the zinc finger was compromised by the various mutations, we saw a decrease in its function. Research such as this will allow us to determine

which areas of the Sirt 6 protein are vital to its function. This is imperative information in the understanding of how Sirt 6 works and therefore how to use SIRT6 to increase lifespan. Furthermore, the cysteine to tyrosine mutation is present in cancer patients. We hypothesize that further investigation into this mutation, and how to deter it from happening, could be a very useful treatment for cancer patients.

References:

[1] Kanfi Y, Naiman S, Amir G, Peshti V, Zinman G, Nahum L, Bar-Joseph Z, Cohen HY. The sirtuin SIRT6 regulates lifespan in male mice. Nature. **483**, 218–221 (2012) https://doi.org/10.1038/nature10815

[2] Roichman A, Elhanati S, Aon MA, Abramovich I, Di Francesco A, Shahar Y, Avivi MY, Shurgi M, Rubinstein A, Wiesner Y, Shuchami A, Petrover Z, Lebenthal-Loinger I, Yaron O, Lyashkov A, Ubaida-Mohien C, Kanfi Y, Lerrer B, Fernández-Marcos PJ, Serrano M, Gottlieb E, de Cabo R, Cohen HY. Restoration of energy homeostasis by SIRT6 extends healthy lifespan. Nat Commun. **12**, 3208 (2021). https://doi.org/10.1038/s41467-021-23545-7

[3] Pace, Nicholas J, and Eranthie Weerapana. "Zinc-binding cysteines: diverse functions and structural motifs." Biomolecules **4**, 419–434 (2014). https://doi.org/10.3390/biom4020419

[4] *Mutation Overview Page SIRT6 - p.C177Y* https://cancer.sanger.ac.uk/cosmic/mutation/overview?id=105687971.

Influence of Chemotherapy on the Microbiome and Immunological Functioning of the Gut

Eliana Farkas

Advised under Dr. Nissan Yissachar, Sivan Amidror, Shalhevet Azriel, and Ariel Simon

Chemotherapy is one of the primary treatments used to treat cancer. Chemotherapy targets the body's dividing cells, with the hopes being that metastasizing cells will incur most of the damage. However, often, patients experience severe side effects when the chemotherapy targets one's own body. Our body contains a large population of microorganisms, collectively termed the microbiota. This population of beneficial bacteria are critical for basic functioning, such as digestion, protection from other harmful microorganisms, regulating the immune system, and more. Changes to the composition of the gut microbiota (called dysbiosis) is associated with the development of auto-immune diseases, inflammation and cancer. Based on the critical role of the microbiota in regulating immune system function, **we hypothesize that the chemotherapy-disrupted, dysbiotic microbiota participate in the development of chemotherapy-associated inflammation.**

There are several possible theories that can be used to explain how chemotherapy induces the permeability of the gut that leads to symptoms like mucositis. Chemotherapy was shown to directly destroy the cells in the epithelial lining of the gut cells, which are constantly dividing and replacing themselves. This increases gut permeability and induces leaky gut syndrome. Secondly, chemotherapy may potentially alter the gut microbiome in the lumen, allowing the proliferation of more harmful types of bacteria that are more likely to penetrate the tight junctions between the epithelial cells. Previous findings in the lab found that post-chemotherapy microbiota alters gut barrier

functions, compared with pre-chemo microbiota collected from the same mouse/patient. This is likely a result of some altered bacteria.

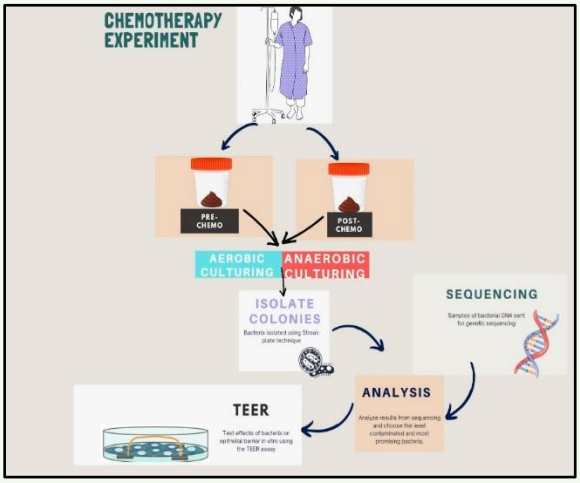

Figure 1. Flowchart of chemotherapy experiment procedure

The aim of this experiment (see Figure 1) is to isolate bacteria from breast cancer patients before and after chemotherapy, to analyze changes to the microbiome and assess their potential exacerbation or therapeutic influence on the epithelium. To accomplish this, fecal samples were collected from breast cancer patients, before and after chemotherapy. The bacteria were cultured and isolated, their genetic material was amplified via PCR (polymerase chain reaction) using primers for the bacterial 16s ribosomal RNA gene, and then sent to sequencing for genetic analysis. The lab will then use the TEER assay to assess the bacteria's altered influence on the tight junctions in epithelial cells. While research is still ongoing, we are hopeful about our hypothesis and our results thus far have been promising.

Establishment of hPSC-based Model for Congenital Kidney Disorder

Sarah Liberow

Advised under Dr. Achia Urbach and Daniella Genet

Congenital anomalies of the kidney and urinary tract, or CAKUT, is a genetic condition that occurs in 1 in 500 live births and accounts for 35% of end-stage kidney disease in children. Most cases of CAKUT stem from disruption of the highly intricate process of organogenesis, leading to defective renal structures. While some mutations have been identified that cause CAKUT, my lab is studying a novel mutation in Gene X, identified in a single young patient suffering from cystic renal dysplasia. Gene X is implicated in the Wnt pathway and was previously not linked to CAKUT.

My work focused on preparing human stem cell lines to closely model the disease as its capacity for self-renewal and ability to adopt any cellular fate make it ideal to study a monogenic disorder such as in Patient X. In order to study loss-of-function of Gene X in human pluripotent stem cells (hPSCs), we explored utilizing the CRISPR-Cas9 system to edit the stem cells' genome. Through both nonhomologous end-joining (NHEJ) and homology-directed repair (HDR), we were able to both create a double knockout of Gene X and work toward inducing a targeted mutation, respectively.

Using nonhomologous end-joining (NHEJ), my lab had edited human embryonic stem cells (hESCs) to knockout Gene X and create partial or complete loss-of-function. In order to differentiate between heterozygous and homozygous knockouts, I extracted and then tested for the protein in the unknown lines versus wild-type and known heterozygotes by performing a Western blot. No protein was visualized in the unknown samples after

development with α-GeneX, while there was protein at the appropriate molecular weight (MW) in the wild-type and heterozygous cells (Figure 1). To confirm that absence of Protein X was due to a double knockout of Gene X, and not due to mishandling of the samples, I developed the Western with α-tubulin to confirm that there was approximately the same amount of housekeeping genes across all samples (Figure 1). Therefore, the evidence supports that the unknown lines are homozygous for the knockout of Gene X.

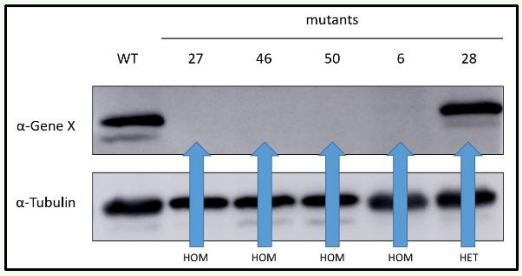

Figure 1: Western blot performed to determine presence of studied protein. No Gene X protein visible in the unknowns and in known homozygous knockout #6. Tubulin is visible in all samples.

Now that we have identified double knockouts for Gene X, the next step was to induce a targeted mutation matching that of our patient so as to compare disease models most closely aligned with the patient. To successfully complete this experiment, we needed to ascertain which guides would lead CRISPR-Cas9 to cut at the correct location upstream of Gene X, which would be followed by homology-directed repair utilizing a template with a deletion of four base pairs in Gene X. My experiment aimed to determine which guide would be the best for this process. I transfected HEK 293T cells with three different guides, as well as a control with GFP to monitor if the transfection was successful. After one day, GFP was visible under fluorescent microscope in about 80-90% of cells, supporting that the transfection had taken place (Figure 2). After extracting and sequencing DNA from the three samples as well as from an additional H9 control, we saw that two out of the three guides were effective at finding and cutting the correct PAM site (Figure 3).

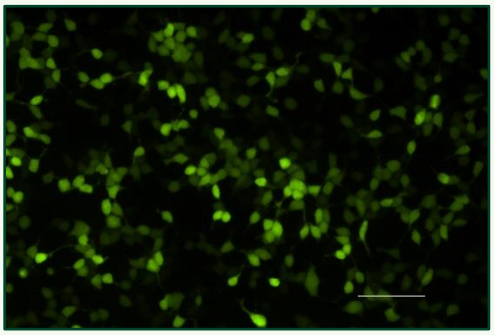

Figure 2: HEK 293T cells control transfected with GFP visualized under fluorescent microscope at 20x.

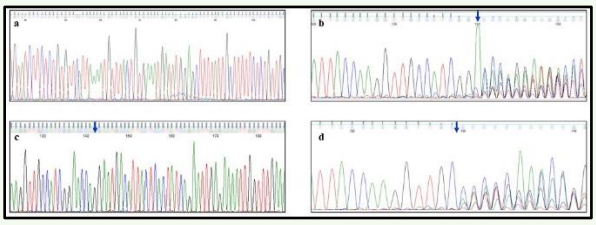

Figure 3: Sequencing data retrieved from transfection. A) H9 control. B-D) Experimental guides

By confirming both heterozygous and homozygous knockouts as well as beginning to identify guides to induce a targeted mutation, our research enables us to learn more about the pathology of this disease and is a step in the development of disease models for Gene X. Using these disease models, we can picture CAKUT *in vitro* which allows for deeper understanding of this novel mutation that causes CAKUT and an expansion of our knowledge on its mechanisms.

Congenital dyserythropoietic anaemia type I (CDA 1); implications of mutations and interactions with proteins Codanin-1 and CDIN 1 (C15Orf41) within diseased individuals.

Eden Shweky

Advised under Dr. Benny Motro

In order for the disease to be studied, understanding the pathways in which they are involved is crucial and thus our project focuses on finding proteins, which physically interact with CDAN1 and CDIN1. Previously, it has been demonstrated that Codanin-1 interacts with the histone chaperon Asf1, suggesting that Codanin-1 (and CDIN1) may be involved in assembly and disassembly of the nucleosomes. CDIN1 (C15Orf41) has been shown to bind to Codanin-1 and to encode to an endonuclease, however, its cellular roles are not clear. In this study, using Crispr methodology, the endogenous Codanin-1 protein was tagged with mCherry, or with FLAG, and CDIN1 was tagged with HA-tag. To try to understand the connection between the two proteins, cells depleted of Codanin-1 were examined for CDIN1 protein levels. The results showed that CDIN1 does in fact disappear with the respective removal of Codanin-1, suggesting that Codanin-1 stabilizes CDIN1.

Manipulated cells expressing the tagged Codanin-1 were used to verify a putative interaction of Codanin-1 and a protein designated APE1 which is involved in the repair of oxidative base damage. PAE1 was overexpressed in cells expressing the endogenous FLAG tagged Codanin-1 and Codanin-1 was then precipitated using antibodies against FLAG after which the co-precipitation of PAE-1 was examined.

In a similar project, I attempted to verify a suspected interaction between Codanin-1 and a protein called SPDL1 or "spindly". SPDL1 is a protein implicated in the interaction between the kinetochore and the spindle microtubules. Professor Andrea Musacchio from Max Planck Institute, a researcher working with this protein was contacted and supplied us with a SPDL1 protein construct. However, as the supplied construct was aimed at bacterial expression, the spindly DNA had to be transferred through a process of three steps of ligations and transformations to a mammalian expression vector. The results of this endeavor are expected to be confirmed by the final construct within the next few days and we will be able to determine whether or not interaction between SPDL1 and Codanin-1 were confirmed.

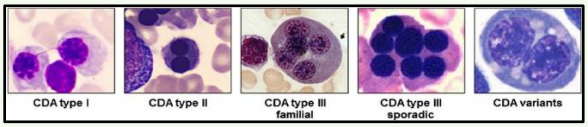

Figure 1. Pathogenic erythroblasts in the bone marrow. Bone marrow erythroblast morphology in different types of CDA

Developing a New Donor Plasmid to Correct RAG1 SCID

Tova Wax

Advised under Dr. Ayal Hendel, Dr. Adi Tovin, and MSc students Bryan Itkowitz and Dor Breier

Severe Combined Immunodeficiency (SCID) is a group of disorders in which patients have severe defects in lymphocytes activity. These disorders are caused by mutations in one of multiple genes. One of those genes is Recombination Activating Gene 1, *RAG1*. The *RAG1* gene encodes the RAG1 protein which is part of the RAG complex. The RAG complex is required for T and B cell maturation, as it is part of the recombination process required to maintain the diversity of their receptors. Therefore, patients with RAG1 mutations have a nonfunctional immune system, and without treatment infants are not able to survive long. The conventional treatment for SCID is allogeneic bone marrow

transplant which, while effective, holds severe risks, such as graft versus host disease (GvHD). Transplantation of hematopoietic stem and progenitor cells (HSPCs) from the patient himself that have been genetically corrected can be a possible alternative cure for this disorder.

Dr. Ayal Hendel's lab aims to find a solution to this disorder using a targeted genome editing approach, altering the DNA sequence of the HSPCs. This can be done using the revolutionary technology of CRISPR, Clustered Regularly Interspaced Short Palindromic Repeats, to attempt and fix the mutated gene. The CRISPR system is composed of a guide RNA (gRNA) and the Cas9 nuclease protein. The Cas9 is directed to a specific spot on the genome using a Watson-Crick base pairing with the gRNA. The nuclease protein, Cas9, creates a double-stranded break (DSB) in the DNA at the target site. There are two pathways the cell can repair DSBs: the first way to repair the break is by non-homologous end joining (NHEJ), fusing the ends of the cut sequence together, which usually creates mutations in the form of insertions and deletions (INDELs) at the location of the DSB. The other way to repair the genome is by homologous recombination (HR), which functions as a cut and paste tool, essentially replacing the mutated sequence with a normal sequence copied from a matching donor template. HR may be used to cure SCID along with other disorders, by introducing a correct copy of the gene into the DSB by using a corrective donor template.

My project in Dr. Hendel's lab was to construct a new donor plasmid that could be used as a template to correct the defective *RAG1* gene in HSPCs by using the HR mechanism. First, the plasmid was designed, and the primers required for its assembly were ordered. Once the primers arrived, PCR conditions were calibrated to determine the optimal annealing temperatures and conditions for each reaction. After the required segments were amplified, they were evaluated on an agarose gel, from which the proper bands were cut and purified. The purified segments were quantified using a NanoDrop and a Gibson reaction was performed to assemble the segments in the proper order, and ligating them with a precut backbone, thus forming the desired plasmid. Once the plasmid was constructed, it was introduced into bacteria by transformation, and the bacteria were seeded on plates containing ampicillin. When the bacteria formed colonies on the plate, several colonies were picked and transferred into LB starters that were placed in a shaker overnight for proper growth conditions. The plasmids were then extracted using the Plasmid Miniprep Kit. Following plasmid harvesting, a restriction testing of the plasmids was executed to determine if the plasmids were indeed correct – the plasmids were cut with restriction enzymes and compared to a computer simulation of how they should look when run on an agarose gel. Once the plasmid was found to be correct, it was sent for sequencing to verify the product. If all went well, the plasmid would then be of use by Dr. Hendel's lab in their research to correct the *RAG1* gene and hopefully cure the SCID disorder.

MATHEMATICS

Daniel Elfenbein

Incidence Lattice of Line Arrangements up to 8 Lines Determines the Fundamental Group

Daniel Elfenbein

Advised under Dr. Mina Teicher and Dr. Eran Liberman

An important property of a space is its fundamental group, and one of the open questions of the geometry of line arrangements is to what extent the incidence lattice of a line arrangement determines its fundamental group. Line arrangements of up to 6 lines were recently classified and shown to determine the projective fundamental group (Fan, 1997). Over the course of the summer, I studied a paper written by David Garber, Mina Teicher, and Uzi Vishne in which line arrangements of up to 8 lines are classified. In particular, Fan's result is extended, and it is shown that the incidence lattice of line arrangements of up to 8 lines determines the affine and projective fundamental groups.

ENGINEERING

(L-R) Ezra Wildes, Yair Caplan, Jonathan Haller, Raziel Siegman, Jacob Minkin, Talya Erblich, and Yitzhar Shalom

Gene Interaction Analysis with Abstract Boolean Networks and Formal Verification

Yair Caplan, Raziel Siegman and Jonathan Haller

Advised under Prof. Hillel Kugler

Analysis of gene interaction within cells is a field of significant interest for biologists. It is critical to the understanding of how a gene network will change over time, and how mutations or perturbations of the system will affect network topology and dynamics down the line. Understanding this can give biologists the knowledge to reverse engineer gene networks, and further understand their design and purpose. Human understanding and intuition of network dynamics can be surprisingly accurate, especially for those intimately familiar with a given network. However, there are certainly limitations to human capacity and predictive

capability as a network's size and complexity increase. Therefore, the tools of computational biology must be employed to provide a rigorous understanding of a gene interaction network.

It has become standard to study gene interaction networks by modeling them as Boolean Networks, where each gene is represented as a node that holds one of two binary states (on/off), and interactions between genes (inhibiting or activating) are modeled as signed directed edges between nodes. Often a network contains interactions which, based on experimental observations, scientists think might exist, but there is still uncertainty. To deal with such a network, Abstract Boolean Networks (ABNs) are employed, such that directed edges are flagged as either concrete (if the interaction is known to exist), or optional (if the existence of the interaction is still undetermined). Furthermore, the network can be modeled over time as a dynamic system by using update functions, such that a node's state is determined by evaluating a Boolean expression of its incoming edges' states. Finally, experimental observations of network states at specified time steps are added as empirical constraints to the network topology, to produce a constrained ABN (cABN).

The issue is that these analyses become extremely unwieldy with even modestly sized gene networks, due to the number of possible network states when considering the two critical uncertainties: interactions whose existence have yet to be verified or disproven, and the wide range of possible update functions a given gene might be operating with. Altogether, brute-force searches of such a system would assume a highly impractical factorial runtime. Alternative computational approaches using formal model verification have been successfully applied to reduce runtimes to feasible standards. The BRE:IN tool uses the NuSMV formal verification model checker to identify subsets of the optional interactions which produce satisfiable solutions.

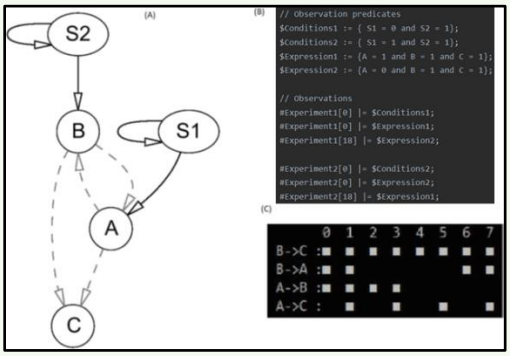

Figure 1: Toy Model: (A) An Abstract Boolean Network with components S1, S2, A, B, C. Four of the interactions A → B, B → A, A → C and B → C are optional interactions that are depicted with dashed lines in the diagram. (B) Experimental observations are specified on the dynamics of the network using an observation specification language defined in RE:IN. (C) After running synthesis, 8 solutions are found to be consistent with all the experimental constraints, they are shown graphically as columns 0 .. 7 highlighting which optional interactions were chosen in each concrete model.

We implemented and tested a number of extensions to the BRE:IN tool, as well as programs built on top of BRE:IN to study specific questions of interest.

Additional functionality was added to BRE:IN to define solution uniqueness by the update functions used for each node, potentially producing multiple solutions with distinct network dynamics for each solution previously identified by BRE:IN. A benefit of this extension is that solutions can be further analyzed and rigorously understood. For example, using our conversion tool, BRE:IN output can now be easily exported and simulated on Boolean Network simulators (such as BooleSim and BoolNet) which utilize rules files (containing update functions) to determine the network state at each time step.

A further modification to BRE:IN we tested was swapping the current NuSMV model checker with the newer version of the tool, nuXMV. Interestingly, after trying multiple algorithms using this alternative, we found that while in certain models, there were modest time

improvements, other models performed slower than its older NuSMV counterpart.

Another question of interest in studying these networks is whether genetic perturbations of the network will produce determinate states for specific genes. For example, one might be interested in knowing whether perturbing a certain gene (or group of genes) will result in the activation or repression of a target gene in the network at a specified point in time. To solve this, we developed the Perturbation Simulator, which makes calls to BRE:IN and processes the result to predict the effects of knockout or overexpression combinations on a target gene. The results obtained from the simulation could then be used to predict the potential effect of mutations on the gene network as a whole.

A final area of interest is the concept of a Minimal Unsatisfiable Core (MUC). An MUC is defined as a subset of experimental constraints which produce a logical contradiction and are therefore mutually unsatisfiable, but produce a formally verifiable solution when any one of the constraints are removed. Identifying an MUC would potentially ease the process of revisiting experimental data when satisfiability is not reached, and simplify the decision of which observations to reconsider. The MUC Identifier we developed acts as a useful tool for this endeavor, as it identifies minimal contradictory sets of complete experiments, and can sub-identify minimal sets of mutually contradictory constraints on the time-step level of granularity.

Further research in the area of formal verification and study of cABN representations of gene network interactions could benefit from: 1) a summarizing tool which produces insights as to the update functions that are most likely to be accurate, 2) a more robust implementation of perturbation prediction which supports even more combinations of knockouts and overexpressions, 3) an algorithm that can identify the globally minimum MUC in a set of experimental constraints, so that the fewest number of observational assumptions need to be revisited, 4) a more intuitive, user-friendly, and insightful output format of BRE:IN models, 5) further experimentation with algorithms provided by nuXMV on a wider variety of models, and 6) a broad, scalable algorithmic approach to the slower processes described above.

Testing a Memory Chip Bit by Bit

Talya Erblich
Advised under Prof. Adam Teman and PhD student Odem Harel

Your computer is pretty awesome. You can use it for many things. However, it cannot work without a memory chip. Without a memory chip, the data that you send into your computer will not have a place to be stored. The information you feed into your computer will instantly be forgotten rendering it completely useless. Through the ages, memory chips have become more and more sophisticated. The size of the chip shrinks, but more data can be held and the chip can operate with less power. The speed that the memory chip operates at also has been decreasing as computer engineers redesign the memory structures and discover new materials that allow memory storage. Over this summer I have had the opportunity to study a memory chip called Leo 1. Leo 1 has a unique design that allows the data inside the chip to be processed faster with an optimized power consumption rate.

Since the design of Leo 1 was already implemented, my project this summer was to troubleshoot why it wouldn't work and then determine optimal voltage levels to maintain the integrity of the data. Using a C code, I was able to simulate the data a user might send into

the chip. Since all information is sent into a computer as 1's and 0's I have been writing codes that send different patterns of 1's and 0's into the chip. Once I write the data into the chip I need to access the data again and read it back to my C code to make sure it is the same as data that I sent in.

Immediately after I began testing the chip I started noticing some strange patterns. Certain sections of the chip would consistently malfunction when sending 1's as data to the entire chip. The opposite sections of the chip would malfunction when 0's were sent as the data to the entire chip. For a while the designer of Leo 1, Odem, and I could not figure out why that specific area was malfunctioning. Eventually we went into the electrical design of the chip and discovered that two of the wires were switched with each other. Because of this, I was writing to one section of the memory chip and then reading back from a completely different section of the chip. Luckily we were able to come up with a temporary solution to the problem using some clever coding tricks but the design of the chip will need to be updated for the next chip, the Leo 2. Below is a picture of the coding adjustment of the wiring.

```
unsigned int rd32_(unsigned int addr) {
    volatile unsigned int t;
    //for (t = 0; t <= 350; t++);

    if (((addr & arr1) != 0) ^ ((addr & arr2) != 0)) { //if we are accessing one of the middle subarrays
        rd32(addr);
        return rd32(addr ^ 0x3000);
    } else {
        return rd32(addr);
    }
}
```

Once this solution was implemented the chip began to work and it was time to test its full capabilities. Normally a memory chip cannot hold data for long as the energy in the chip starts leaking after a few fractions of a second. Odem and I decided it was time to test the amount of time the data can be held in the chip before it all disappears. Computer Engineers call this the retention time. After running some tests we realized that the memory chip prefers to hold 0's longer than 1's. This was not ideal. We wanted our chip to hold both ones and zeros for the same amount of time. To achieve this, we realized that we would need to adjust the power supply levels on our chip. Below is a graph of the retention time from when we sent all 1's to the chip (we call that Data = 0xFFFFFFFF) and the retention time when we sent all 0's to the chip (We call that Data = 0x00000000). You can see that the number of errors goes up the longer we wait between writing the data and reading the data. You will also notice that when we write 1's into the chip, they can last up until 96 microseconds. At that point the memory starts leaking energy and we can no longer guarantee that the chip is 99.99% accurate. When writing the data as 0's the chip was able to maintain above 99.99% accuracy for almost 230 microseconds. While the amount of time a 0 can be held is impressive, the 1's being held would dissipate much faster and it would be more ideal to have a greater retention time for the 1's at the cost of a smaller retention time for the 0's.

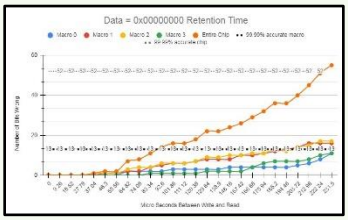

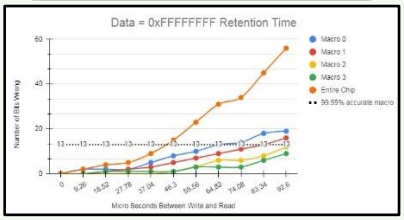

Over the course of this project I learned about the importance of Verilog, the beauty of SimVision, the simple brilliance of C, and the genius and complexity of computer architecture. We take memory devices for granted every day. We understand that they work and we use them without much thought about what goes on under the computer's cover, beneath the keys, and beyond the screen. I am grateful to have spent a summer exploring these devices. I want to send a special thank you to

Odem, Adi, and the rest of the ENICS lab at BIU for helping me learn so much this summer. Lastly, I would like to thank YU for inviting me to this fantastic program. My memories of this summer far surpass the amount of memory available on my chip.

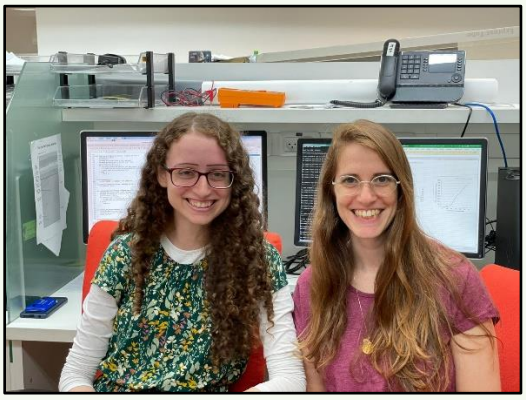

Computer Vision using Residual and Hyper Networks

Jacob Minkin

Advised under Dr. Ethan Fetaya

Imagine a world where cars drive themselves, missiles are guided by computers, and patients are diagnosed by robots. Cars must scan the road in real time, missiles need to track their target, and computers need to analyze x-rays to understand what's wrong with the patient. Using advanced network structures, programmers can design systems that can process real world images using a revolutionary structure called Convolutional Neural Networks (CNNs).

CNNs are deep artificial neural networks. An artificial neural network is a network of nodes that connect input layers to output layers.

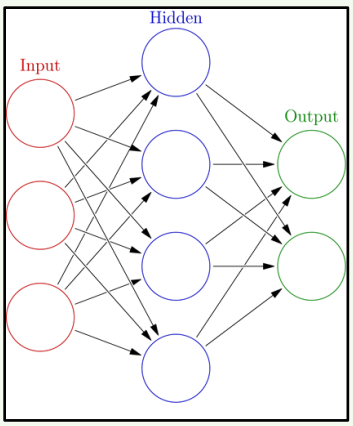

*from Wikipedia

Each circle in the above image represents a node. Each node includes a weight which controls the output of the node. The input layer represents the original image, and the output layer represents a prediction by the network. The hidden layers in between change the image and prepare it for prediction. The hidden layers are composed of three types of layers: convolutional layers, pooling layers, and fully connected layers. A convolutional layer processes the image and scans for important features. It changes the image by emphasizing the important features. A network can have many convolutional layers stacked together. Sometimes the image is too big and requires pooling layers. Pooling layers are used to reduce the size of the image by splitting the image into sections and reducing each section into one pixel. Lastly the fully connected layer generates a prediction vector by analyzing the final image.

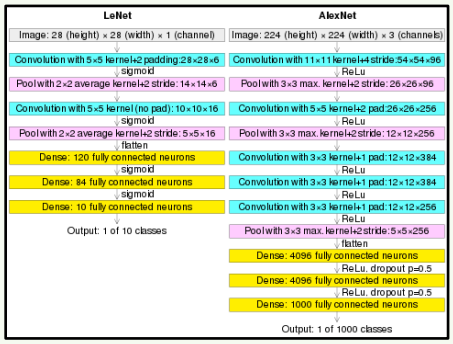

*from Wikipedia

CNNs are trained using a process called backpropagation. The prediction vector from the fully connected layer is compared to the actual classification of the image. It then goes back through the entire network changing all the weights to fit the actual prediction. This process is repeated for every image in the dataset. Through this, the network "learns" how to classify each image.

In 2015 a group from Microsoft Research revolutionized the structure of CNNs. Ideally, adding more layers to a CNN should help it understand deeper features of the image. This would lead to higher accuracy. Instead, larger networks performed worse than smaller networks. This had to do with the zeroing of the weights at high layers of the network. The researchers solved this problem by creating residual networks. Residual networks (ResNets) include identity mappings which saves information from earlier layers. It uses this information to reinforce the weights of later layers. These researchers used residual networks to build one hundred fifty-layer networks with best in the world accuracy.

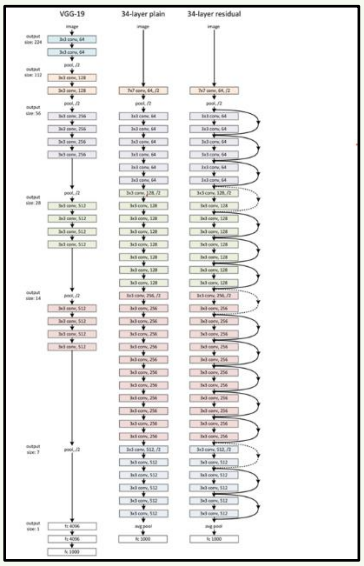

*He, 2015

The large size of residual networks makes it slower to train. So, in 2016 researchers at Google Brain introduced the hypernetwork. Hypernetworks are small networks that train the weights of a second larger network called a target network. They compare hypernetworks to the genotype – phenotype relationship in biology. The hypernetwork, which is the genotype, can adjust the target network, which is the phenotype based on the input or environment. Using hypernetworks is more efficient then training the weights of a larger network. This is because hypernetworks have less weights which helps maximize training efficiency and space.

In my research, I am using a hyper network along with two residual networks. Residual networks can correctly classify an image seventy percent of the time. If you give the network five guesses, its accuracy goes up to ninety percent. To increase the top line accuracy, the hypernetwork takes the top five predictions of the first residual network and uses it to design a second residual network that specializes in distinguishing between those top five. Hopefully this second network will return more accurate results than the first network.

The Enhancement of Cisplatin Treatment of Resistant Cell Lines Via Glucose-Linked Gold Nanoparticles

Yitzhar Shalom

Advised under Prof. Rachela Popovtzer and Dr. Yoray Sharon

The efficacy of the chemotherapy drug cisplatin is significantly undermined by the various mechanisms through which cancer cells develop resistance to the drug. One postulated mechanism of resistance is the exposure-induced reduction in the expression of CTR1, the

surface receptor responsible for mediating the entry of the drug into the cell. Once in the cell, the drug is modified to a toxic form that attaches to adenine and guanine base pairs in DNA, introducing kinks in the secondary structure that impede replication. Hypothetically, therefore, cells that have adapted to downregulate CTR4 are less susceptible to the toxicity of the chemotherapy treatment.

Our project aims to bypass this mechanism of resistance by inducing entry through an alternate pathway. To do this, we synthesize gold-nanoparticles (GNPs) of 20 nm in diameter and conjugate them to cisplatin via a PEG 1,000 linker. GNPs have previously been demonstrated to be effective, nontoxic, nonimmunogenic vehicles for drug delivery [1]. We also attach glucose, the ligand of surface glucose transporters. The purpose is for the complex to enter the cell through a different route such that the CTR1 pathway is bypassed, and the treatment will still be detrimental to cells that have become naturally resistant.

To test this model, we generate resistant cells by continuously incubating strains of renal and bladder cancer cells with increasing quantities of cisplatin, allowing recovery time in between subsequent drug treatments. Once the cells are determined to have achieved sufficient resistance, we apply our synthesized GNP-cisplatin-glucose complex and observe the resulting viability of the cells as they compare to cells treated directly with cisplatin and in comparison to non-resistant cells. Our hypothesis will be supported if the cells treated with the GNP-conjugated chemotherapy will result in greater cell death than non-conjugated cisplatin.

References:

[1] Brown, S. D. et al. Gold nanoparticles for the improved anticancer drug delivery of the active component of oxaliplatin. J. Am. Chem. Soc., **132**, 4678–4684 (2010).

https://doi.org/10.1021/ja908117a

Textual Structure Analysis and Bold Detection Using OCR

Ezra Wildes

Advised under Joshua Guedalia

Since the invention of the printing press, hundreds of millions of books have been published. For centuries earlier, an untold number of books were written, transcribed and disseminated. Contained within these books are the collective wisdom and stories of humanity. Since the beginning of the 20th century, scientists have attempted to create mechanisms to digitize these texts and analyze their contents. The field of Optical Character Recognition (OCR) utilizes state-of-the-art advances in computer science – such as machine learning, computer vision, and neural networks – to automate the process of converting handwritten and printed pages into digital, machine readable text.

The process of OCR begins with pre-processing the image to optimize the text readability. This includes page alignment through various deskewing techniques, binarization of an image to separate the text from background information and convert the image to black-and-white, and other methods of image cleaning. Then, the image is broken up into glyphs, a representation of a character still unidentified, and various mechanisms are utilized to accurately determine the correct character that the glyph represents. One simple method is called matrix matching, where the computer has

a database of matrices representing the pixel structure of all of the potential characters and compares them to the matrix of the glyph to determine the most likely match. However, this method can easily be ineffective when the image uses a different font of a less-readable text, so another mechanism called feature extraction was developed. Significant features about the structure of the character are determined and compared to an abstract representation of a character with given features to determine the match. Then, post-processing techniques are used to improve the output of the program by using a defined list of possible words and numerous algorithms which utilize the frequency of word combinations and an understanding of the language grammar to increase the accuracy of the resultant text.

While much advancement has been made in OCR technology, less work has been done in determining the textual structure of a document. Such accomplishment can allow detection of various structural characteristics of a document – including bolded text and headers – which can allow for an organization and even understanding of the text.

Working for Dicta – a non-profit organization which specializes in using "cutting edge machine learning and natural language processing tools to the analysis of Hebrew texts"[1] – I was tasked with advancing algorithms that can accurately determine the text structure and bold characters from both ancient and recent Hebrew manuscripts.

Using OCR programs, I was able to isolate hundreds of thousands of characters, from dozens of pages, and automate the process of labeling them as being bolded or not. By analyzing a whole host of characteristics, or features, I was able to use CatBoost, a "machine learning algorithm that uses gradient boosting on decision trees" [2], to train a machine learning model with 99% accuracy of bold detection. Then, using SHapley Additive exPlanations (SHAP)," a game theoretic approach to explain the output of any machine learning model", I was able to create visualizations for and determine the relative impact of each feature of the text upon the model and adapt its particular features to solve the specific problem of identifying bold words in Hebew manuscripts – thus creating an effective model in determining the boldness of Hebrew characters and, ultimately, text structure.

References:

[1] https://dicta.org.il/about

[2] https://shap.readthedocs.io/en/latest/index.html

PHYSICS

(L-R) Luna Kadysz and Charles Grill

Magnetization Switching and its Impact on Spintronics

Charles Grill

Advised under Prof. Amos Sharoni, and Master's Student Lior Saadia

In the field of spintronics (the study of utilizing quantum spin in electronics), there is a quantum phenomenon called magnetization switching. This is a phenomenon in which the magnetic field produced by a certain oriented ferromagnetic sample can switch directions. This is done via an induced electric current and an external magnetic field being applied to the sample. This magnetization switching has huge effects and impacts on the technological industry of data storage, allowing for more physical data storage in a smaller confined space (in the magnitude of nanometers). This was

previously impossible due to the quantum effects like quantum tunneling that would occur at that magnitude. Utilizing magnetization switching in transistors and circuits we can distinguish bits without encountering these effects allowing us to minimize our components to smaller magnitudes and have faster computing. My research this summer was to conduct experiments and see which compositions of our ferromagnetic samples yielded the most efficient results for this magnetization switching. To study this and find more efficient samples we experimented on custom ferromagnetic materials which we synthesized in our lab using a sputtering machine. The sputtering machine allowed us to build our samples by depositing specific elements and materials layer by layer on a molecular scale onto a clean SiO2 Substrate. We then bonded our samples to a PCB test board and tested them in our Closed Circuit Refrigerator (CCR). The CCR is a multipurpose testing machine that allows for a variety of testing for the samples in our lab. We studied our completed samples and their properties by applying the anomalous hall effect via CCR and gradually changing the external magnetic field from 2000 to -2000 Oersted. This was done in order to calculate our perpendicular magnetic anisotropy (PMA) measurement. This PMA measurement shows us the change in the hall voltage as the external magnetic field changes. The PMA measurement is the key to observing magnetization switching and if there is a hysteresis on the measurement graph then magnetization switching conditions are met. We did these tests on different samples with different compositions using materials such as Palladium, Cobalt, Iron, Boron, and Platinum to see which samples yielded the most efficient results and improve the already established data.

Landscape Static Measurement Predicts Wave Localization in Complex Structures

Luna Kadysz

Advised under Prof. Patrick Sebbah and Dr. Eitam Luz

A particular phenomena exhibited in complex or irregular systems is their ability to maintain standing waves in confined subregions of their domain in the presence of arbitrary forces or potentials. Here, we study a newly-discovered method for extracting these localized modes of an irregular plate.

The model is based on the recent development of a mathematical theory of quantum localization, which introduces for each type of carrier a spatial function called localization landscape. These landscapes allow us to predict the localization regions of vibration modes in complex or disordered systems.

This paradigm captures two major effects of quantum mechanics – the tunneling effect and the quantum confinement effect – without having to solve the Schrödinger equation, which implies a major computational breakthrough.

In previous studies [1] the model was applied to several one-dimensional structures, where comparisons with exact Schrödinger calculations demonstrate the excellent accuracy of the approximation provided by the landscape theory.

Here, we aim to explore the localization landscape in a two-dimensional structure. Studying a two-dimensional plate with complex geometry provides direct access to the landscape function and demonstrates its predictive power.

[1] Localization landscape theory of disorder in semiconductors, M. Filoche, M. Piccardo, Y. Wu,

C. Li, C. Weisbuch, and S. Mayboroda. Phys. Rev. B **95**, 144204 (2017).

https://doi.org/10.1103/PhysRevB.95.144204

[2] One single static measurement predicts wave localization in complex structures, G. Lefebvre et al., Phys. Rev. Lett. **117**, 074301 (2016).

http://dx.doi.org/10.1103/PhysRevLett.117.074301

CHEMISTRY

(L-R) Mili Chizhik and Yael Laks

Using UV-Vis Spectrophotometry for the Optimization of the Conditions of G-quadruplex-MP-11 Complexation Reactions

Mili Chizhik

Advised under Dr. Eyal Golub and Dr. Nurit Adiram

The interactions between nucleic acid sequences and proteins are of utmost importance for life-sustaining processes in all organisms. However, each interaction requires a different set of environmental conditions, surroundings, and wide-ranging molecular resources to successfully complete the desired mechanism. One such example of a protein interacting with a sequence of nucleic acids is the guanine-rich quadruplex that binds with different types of proteins.

Guanine-rich quadruplexes, or G-quadruplexes, is one example of a nucleic acid secondary structure. The G-quadruplex is made from a tetrad of guanines that interact via π-π stacking and Hoogsteen-type hydrogen bonds [1]. The structure is further stabilized by monovalent metal ions, primarily potassium ions (K^+) that are positioned in between the tetrads. The topology of the G-quadruplex varies greatly and can fold either into parallel, antiparallel, or hybrid structures and can form either inter- or intramolecularly. [2] The topologies can be identified by various biophysical methods via the analysis of the circular dichroism spectrum of each sequence and compared with known

signals that are distinctive of the specific topologies.

Microperoxidases are heme-containing catalytic peptides that break down the cellular respiration's byproduct of hydrogen peroxide, and they have been determined to be the products of the proteolytic breakdown of cytochrome c, with microperoxidase-11 (MP-11) being the most well-known heme-peptide [3]. This eleven amino acid heme-peptide is bound to a metalloporphyrin through the coordination of the histidine-18 residue and the iron cation.

This research is repurposing MP-11 to be a model for the G-quadruplex-microperoxidase interactions while also creating a simpler way to monitor the complexation reaction. This is because heme has characteristic spectral changes that accompany the complexation of itself and G-quadruplexes. G-quadruplexes are biochemically relevant and their interactions with MP-11 have not yet been closely examined; therefore, the optimization of the environmental conditions of the different reactions must first be achieved to continue to explore these compounds. The results from varying the buffer solutions used can illustrate the interactions between the solvent components and the aggregation of the MP-11, as well as the complexation with G-quadruplex. However, the varying of the G-quadruplex sequences will demonstrate how closely binding the G-quadruplex-MP-11 complex is and the specificity of the sequence based on its topology.

Initially the MP-11 was added to the solution and then once the G-quadruplex was added, the histidine residues and positively charged iron cation in MP-11 bound to the negatively charged G-quadruplex sequence and the height and width of the peaks varied depending on sequence and buffers used, as predicted. One of the two spectral peaks can clearly be seen, and the height and width vary with the different solute and solvent conditions. For example, one can see two peaks in Figure 1, one associated with the MP-11 aggregation prior to the addition of the G-quadruplex and the second peak is associated with the G-quadruplex-MP-11 complex. The peak not shown in the figures corresponds to the charge-transfer peak for the complex. The hyperchromicity of the shown peak is an indicator of the hydrophobic nature of the [EG1] interaction between the MP-11 and the G-quadruplex. Similarly, one can see the varying nature of the complexation reactions with the different G-quadruplexes and buffers in Figures 2 and 3.

Through the optimization of the complexation reactions, one can utilize the data obtained to further our understanding of the interactions between the G-quadruplex and the MP-11. Since G-quadruplexes are prevalent in the telomeric regions of the chromosomes and the promoter region within the oncogenes, they have a very important role in transcriptional regulatory processes and anti-cancer treatments, such as chemotherapy and drugs with high selectivity. Thus, researching the optimal conditions under which we can identify and select for the G-quadruplex can have major basic and translational science and clinical applications especially into the molecular basis of the development of diseases.

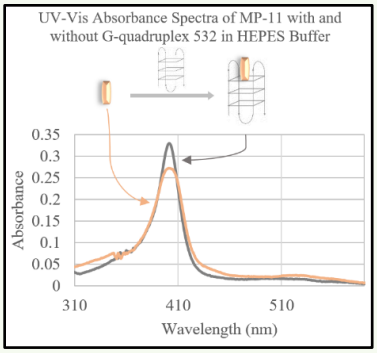

Figure 1: UV-Vis Absorbance Spectra of MP-11 with and without G-quadruplex 532 in HEPES Buffer. Two peaks can be seen in the

absorbance spectra: the orange-colored peak represents the absorbance associated with the aggregation of the MP-11, whereas the grey-colored peak is the peak associated with the complexation of the 532 G-quadruplex with MP-11. Above the spectra, a simplified illustration of the complexation reaction can be seen with the arrows pointing to the corresponding peaks.

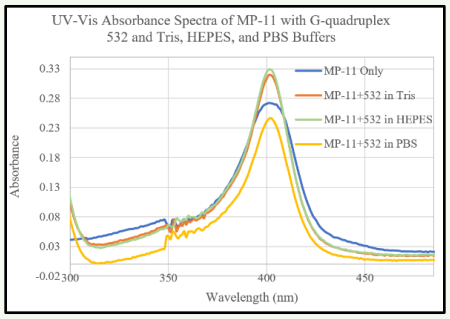

Figure 2: UV-Vis Absorbance Spectra of MP-11 with G-quadruplex 532 and Tris, HEPES, and PBS Buffers. Four peaks can be seen from the different complexation reactions in the different buffers.

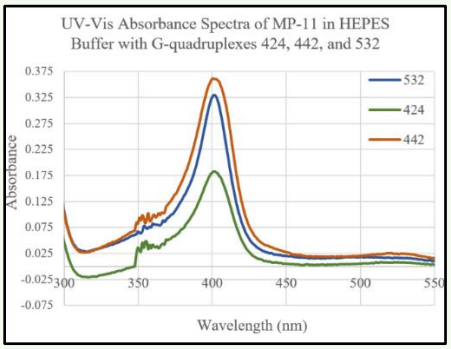

Figure 3: UV-Vis Absorbance Spectra of MP-11 in HEPES Buffer with G-quadruplexes 424, 442, 532. The three peaks shown in the spectrum correspond to different G-quadruplexes used and illustrate the difference in complexation characteristics of their unique topologies.

References:

[1] McRae, Ewan K. S., et al. “On Characterizing the Interactions between Proteins and Guanine Quadruplex Structures of Nucleic Acids.” Journal of Nucleic Acids, **2017**, 9675348 (2017).

https://doi.org/10.1155/2017/9675348

[2] Golub, Eyal, et al. “Metalloporphyrin/G-Quadruplexes: From Basic Properties to Practical Applications.” Journal of Porphyrins and Phthalocyanines, **19**, 65–91 (2015).

https://doi.org/10.1142/S1088424615300025

[3] Verbaro, Daniel, et al. “Microperoxidase 11: A Model System for Porphyrin Networks and Heme–protein Interactions.” Journal of Biological Inorganic Chemistry, **14**, 1289 (2009).
https://doi.org/10.1007/s00775-009-0574-9

The Structural Organization of the CopY Metalloregulator

Yael Laks

Advised under Prof. Sharon Ruthstein and research student Melanie Hirsch

Keeping organisms in a proper state of homeostasis is critical in order to maintain survival. Specifically, metal ions such as copper, in appropriate concentrations promote necessary cellular processes. The copper cycle plays a crucial role in prokaryotes because copper ions are required as cofactors for enzymes that catalyze oxidation reduction reactions, as well as assisting in regulating DNA transcription within the cell. When proteins involved in the cycle bind to the specific metal ion, it induces changes in structure which either promotes or prevents DNA binding and therefore, regulates the transcription process. In high concentrations, metal ions are proven to be lethal to organisms. Therefore, the Ruthstein lab is studying a more thorough understanding of the biological pathways of copper in order to ensure copper homeostasis in bacteria. Through electron paramagnetic resonance (EPR) spectroscopy and computational modeling, a proper structure-function understanding of the systems will eventually aid in the future development of inhibitors. These inhibitors could be ultimately incorporated into a new generation of antibiotics. These drugs will expectantly work to kill the bacteria while ensuring the safety of another organism’s host.

Under the guidance of Melanie Hirsch, the function and efficacy of the copper metoregulator, CopY is analyzed in *S. pneumoniae*. Metalloregulators are transmembrane or cytoplasmic proteins that bind to specific metal ions with high affinity and play a role in regulating the concentration of the ions within the cell. CopY, a transcription factor, is able to induce or repress the expression of specific genes through metal binding. Structural information is lacking for this protein in *S. pneumoniae*, limiting the ability to elucidate the mechanisms of function, although it has been previously identified and characterized in *Enterococcus hirae*. In past research determined by NMR spectroscopy, the DNA binding domain was identified as a canonical winged-helical motif. CopY from *S. pneumoniae* has three Cys residues which can be spin-labeled (Figure 1).

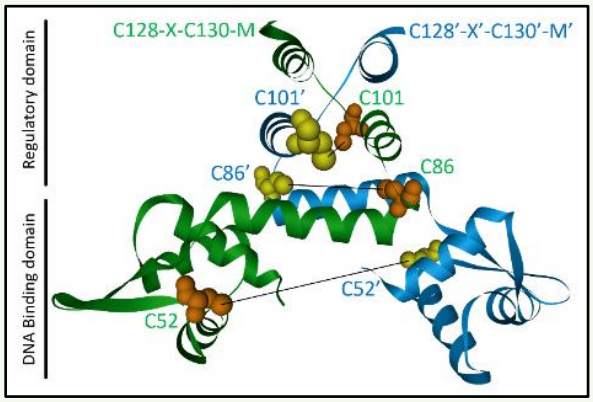

Figure 1: S. pneumoniae CopY protein model structure. The model was created with SWISS-MODELELR based on the methicillin regulatory protein (PDB 1OKR). Cysteine residues that are available for spin labeling to EPR measurements are marked.

Naturally, CopY is a dimer that either binds Cu(I) ions or binds to Zn(II) in a repressor state. At a certain threshold concentration of copper in the cell compared to zinc, two molecules of Cu(I) will replace the zinc molecule. The protein adapts its conformation and releases the DNA binding site, expressing the DNA strand attached. If the DNA is expressed, a feedback mechanism loop occurs by translating copper chaperones CupA and Cu-effluxes CopA, which are involved in restoring proper copper concentrations within the cell.

Before I came, the wild type protein was previously expressed. The research I became involved with began by studying mutations on the wildtype at position C86. In order to obtain the protein structure and function, biomolecular techniques such as PCR, Ni resin protein purification, EMSA and crosslinking were performed (Figure 2).

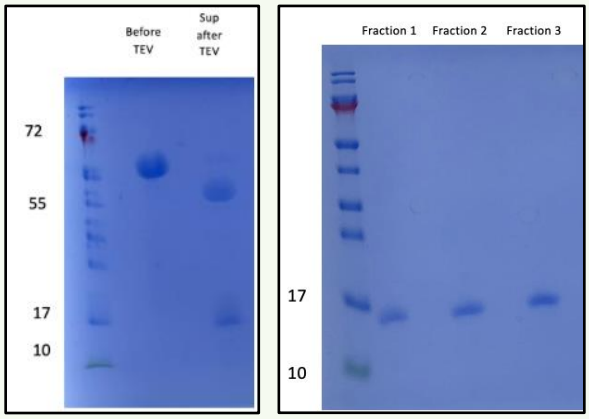

Figure 2. Gel image of purified protein once cut with TEV

In order to study the protein structure and behavior with varied concentrations of Cu(I) and Zn(II), the Ruthstein lab EPR spectroscopy. A type of EPR used is continuous wave (CW) spectroscopy. The protein was spin-labeled with MTSL, a nitroxide paramagnetic probe that can be attached to cysteine residues in the protein. This was done in order to confirm the protein was spin-labeled correctly. Additionally, dynamics of the side chains changed. This means the ion is bound and a change from the wild type was observed (Figure 3). Based on the peaks, when concentrations of copper and zinc varied, a change in the dynamics of the side chains additionally changed. In addition to CW, double electron-electron resonance (DEER) will be utilized. DEER is a type of pulsed EPR spectroscopy. This works through isolating the electron-electron dipolar interaction between two spin probes stimulated by a set of pulses.

Data obtained can be used to extrapolate calculations that can measure distances at the nanometer range 1.5-8.0 nm. This approach is valuable and distinctive as it can study proteins with different sizes, informing about the inter-monomer distance and changes. In order to observe if the protein changed once the specific mutation was done, the distance between C86' and C86 will be measured.

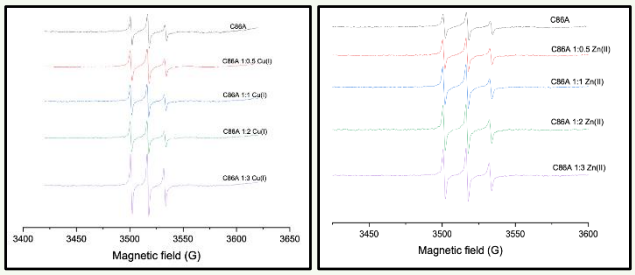

Figure 3. CW EPR spectroscopy graphs. Left is Cu (I), right is Zn (II).

Combining these biomolecular techniques and computational modelling, the protein general structure and function can be solved.

References:

Casey, Thomas M., and Gail E. Fanucci. "Spin Labeling and Double Electron-Electron Resonance (DEER) to Deconstruct Conformational Ensembles of HIV PROTEASE." *Methods in Enzymology*, **564**, 253–187 (2015). https://doi.org/10.1016/bs.mie.2015.07.019

Glauninger, Hendrik, et al. "Metal-Dependent Allosteric Activation and Inhibition on the Same Molecular Scaffold: The Copper Sensor Copy from Streptococcus Pneumoniae." *Chemical Science*, **9**, 105–118 (2018).

https://doi.org/10.1039/C7SC04396A

Samanovic, Marie I., et al. "Copper in Microbial Pathogenesis: Meddling with the Metal." *Cell Host & Microbe*, vol. 11, no. 2, 2012, pp. 106–115.
https://doi.org/10.1016/j.chom.2012.01.009.

Solioz, Marc. "Copper Disposition in Bacteria." *Clinical and Translational Perspectives on WILSON DISEASE*, pp. 101–113 (Academic, 2019). https://doi.org/10.1016/B978-0-12-810532-0.00011-2